

# Dispersion of High-Purity Semiconducting Arc-Discharged Carbon Nanotubes Using Backbone Engineered Diketopyrrolopyrrole (DPP)-Based Polymers

Ting Lei, Gregory Pitner, Xiyuan Chen, Guosong Hong, Steve Park, Pascal Hayoz,\*  
Ralf Thomas Weitz, Hon-Sum Philip Wong, and Zhenan Bao\*

The isolation of semiconducting single-walled carbon nanotubes (sc-SWNTs) with ideal diameter and high purity is highly desired for high-performance electronic devices. However, current sorting methods for large-diameter sc-SWNTs suffer from either low purity (<99%) or long processing time (>20 h). Here, a backbone-engineering strategy is reported for the polymer used for sorting to improve the purity of sorted sc-SWNTs. Six diketopyrrolopyrrole (DPP)-based conjugated polymers are used to systematically investigate their sorting ability for sc-SWNTs. It is found that incorporation of more thiophenes building blocks in the repeating units of DPP polymer backbone leads to increased selectivity and yield for sc-SWNTs. The DPP polymers can disperse sc-SWNTs with 1.4–1.6 nm in diameter and high purity of 99.6% by a processing time as short as 1 h. Furthermore, a scalable film coating method named “solution shearing” is used to fabricate SWNT network thin-film transistors (TFTs). The TFT devices exhibit both high mobilities over  $50 \text{ cm}^2 \text{ V}^{-1} \text{ s}^{-1}$  and high on/off ratios over  $10^5$ , which are among the highest performance for solution-processed SWNT network TFTs.

## 1. Introduction

Single-walled carbon nanotube (SWNT) is a promising material for future electronic and optoelectronic applications<sup>[1]</sup> due to its ultrathin body, ballistic transport,<sup>[2]</sup> outstanding infrared absorption,<sup>[3]</sup> and high mechanical flexibility.<sup>[4]</sup> However, large-scale produced SWNTs are mixtures of semiconducting SWNTs (sc-SWNTs) and metallic SWNTs (met-SWNTs). They are not suitable for direct fabrication of high-performance electronic devices.<sup>[5]</sup> To overcome this issue, various approaches have been developed to selectively remove metallic tubes from commercial SWNTs,<sup>[6]</sup> such as density gradient ultracentrifugation (DGU),<sup>[7]</sup> column chromatography,<sup>[8]</sup> dielectrophoresis,<sup>[9]</sup> deoxyribonucleic acid wrapping,<sup>[10]</sup> and conjugated polymer wrapping.<sup>[11]</sup> Recently, Tulevski et al.<sup>[12]</sup> pointed out three key requirements for a sorting

method targeting at high-performance computing: (1) high-purity semiconducting carbon nanotubes with met-SWNTs <1 ppb are needed for large-scale integration of billions of transistors; (2) large-diameter sc-SWNTs (>1.2 nm) have small Schottky barrier and high drive current;<sup>[13]</sup> and (3) the diameter distribution of sc-SWNTs will affect the resulting threshold voltage ( $V_t$ ), but larger diameter (>1.4 nm) can lessen the variation of  $V_t$ .<sup>[12]</sup> To meet the above requirement, sc-SWNTs with diameters close to 1.7 nm are considered ideal.<sup>[12]</sup> Recently, high purity isolation ( $\approx 99.9\%$ ) of  $\approx 1.4$  nm sc-SWNTs was achieved by column chromatography method.<sup>[14]</sup> However, this method requires multiple steps, several iterations, and long processing time (>20 h). Hence fast and high-purity dispersion of sc-SWNTs with diameters close to 1.7 nm still remains challenging.

Conjugated polymer wrapping has emerged as an efficient, low-cost, and scalable strategy for enriching sc-SWNTs.<sup>[11,15]</sup> The diversified molecular structures of conjugated polymers enable great opportunities to selectively disperse sc-SWNTs with different diameters and chiralities,<sup>[11b,16]</sup> as well as promising applications of sc-SWNT/conjugated polymer hybrid materials.<sup>[17]</sup> However, only a few conjugated polymers showed the ability to disperse large-diameter sc-SWNTs (>1.2 nm) and they mainly disperse 1.3 nm sc-SWNTs with a very low yield

Dr. T. Lei, Prof. Z. Bao  
Department of Chemical Engineering  
Stanford University  
Stanford, CA 94305, USA  
E-mail: zbao@stanford.edu

G. Pitner, Prof. H.-S. P. Wong  
Department of Electrical Engineering  
Stanford University  
Stanford, CA 94305, USA

X. Chen, Dr. S. Park  
Department of Materials Science and Engineering  
Stanford University  
Stanford, CA 94305, USA

Dr. G. Hong  
Department of Chemistry  
Stanford University  
Stanford, CA 94305, USA

Dr. P. Hayoz  
BASF Schweiz AG, GMV/BE  
Schwarzwaldallee 215, 4002 Basel, Switzerland  
E-mail: pascal.hayoz@basf.com

Dr. R. T. Weitz  
BASF SE, GMV/T  
Carl-Bosch-Strasse 38, 67056 Ludwigshafen, Germany



DOI: 10.1002/aelm.201500299

for sc-SWNTs  $>1.4$  nm.<sup>[11d,e,16]</sup> Even fewer polymers can disperse large-diameter sc-SWNTs with high purity  $>99\%$ .<sup>[11c]</sup> Even though some reported estimated purity by spectroscopic method, it is known that this can overestimate the purity due to the complicated nature of SWNT absorption spectrum.<sup>[14,18]</sup> Direct electrical measurement of single tubes is considered to provide more precise information about electronic purity.<sup>[18,19]</sup>

In our previous work, we have shown that diketopyrrolopyrrole (DPP)-based low bandgap polymers are capable of dispersing SWNTs with diameters mainly around 1.5 nm and good selectivity for sc-SWNTs.<sup>[20]</sup> Here we present further investigation of molecular design strategy to increase the selectivity for larger-diameter and semiconducting SWNTs through rational polymer backbone engineering of DPP-based polymers (Figure 1a). The purity and chirality of our polymer-dispersed sc-SWNTs were examined by several spectroscopic methods. We conducted electrical measurements for our sorted high-purity sc-SWNTs using short channel (400 nm) field-effect transistors (FETs). Eighteen to twenty one devices containing  $\approx 150$ –270 sorted SWNTs were tested for different sorting methods. We found that our backbone-engineered DPP polymers can disperse 1.4–1.6 nm large-diameter sc-SWNTs with high purity  $>99.6\%$  and a processing time as short as 1 h. This is one of the highest purity reported to date for polymer sorted large-diameter sc-SWNTs characterized by direct electrical measurement.<sup>[11,16]</sup> Using a scalable solution coating method “solution shearing,” thin film transistors (TFTs) with high mobilities over  $50$  cm<sup>2</sup> V<sup>-1</sup> s<sup>-1</sup> and high on/off ratios over  $10^5$  are demonstrated.

## 2. Result and Discussion

### 2.1. Polymer Design and Selective Dispersion of Large-Diameter SWNTs

Previous theoretical studies have shown that the selectivity of conjugated polymer sorting originates from the  $\pi$ - $\pi$  interactions between the conjugated polymer backbone and SWNTs.<sup>[21]</sup> Compared with sc-SWNTs, met-SWNTs have a higher tendency to form charge transfer complexes with conjugated polymers.<sup>[21a]</sup> The more polar charge transfer complexes tend to aggregate or bundle in nonpolar solvents typically used for sorting and form sediment after centrifugation, leaving sc-SWNTs in the supernatant.<sup>[22]</sup> We therefore hypothesize that a stronger polymer backbone and SWNT interaction may help to enhance the charge transfer interactions and thereby improve the selectivity for sc-SWNTs. To verify this hypothesis, density functional theory (DFT) calculations were performed to compare the interactions between different types of DPP monomers and met-SWNT (18,0) ( $d = 1.45$  nm) (Figure 1b). Compared to DPP3T (three thiophenes in backbone)/SWNT complex, DPP4T (four thiophenes (4Ts) in backbone)/SWNT complex showed a smaller calculated  $\pi$ - $\pi$  stacking distance. The association energy of DPP4T/SWNT complex was calculated to be  $48.7$  kcal mol<sup>-1</sup>,  $10.1$  kcal mol<sup>-1</sup> larger than that of DPP3T/SWNT complex. DPP4T contains 17% more atoms than DPP3T but provides 26% stronger interactions with SWNT, suggesting a synergistic effect in the intermolecular interaction of DPP4T/SWNT complex. Based

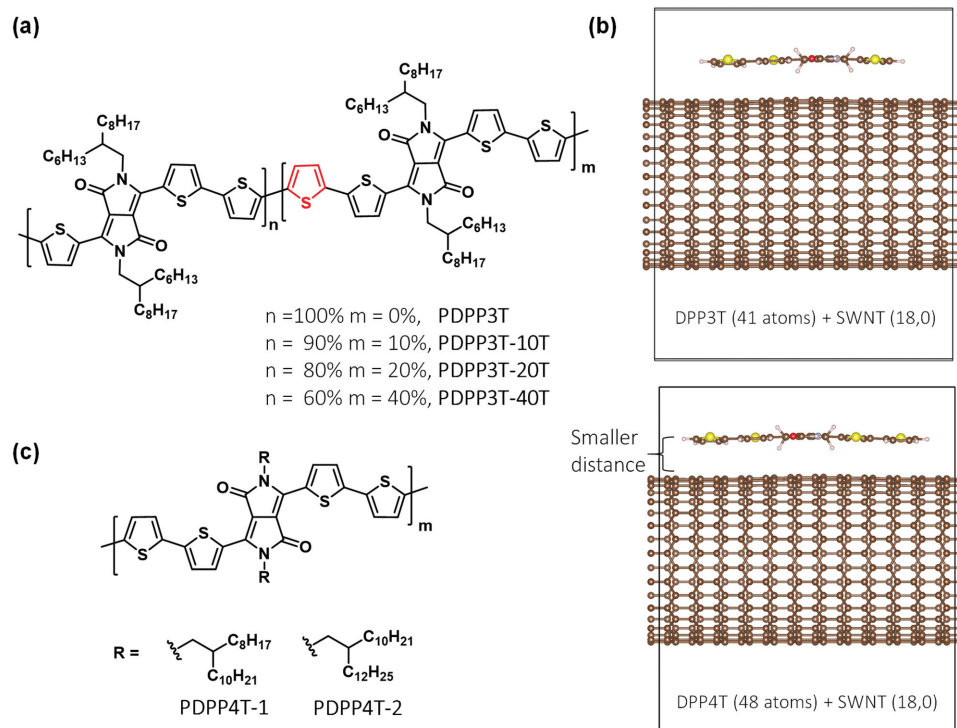


**Figure 1.** Polymer structures and computational study. a) Varying the backbone structure of DPP-based conjugated polymers by introducing different amounts of thiophene units. b) DFT study on the interaction between different DPP monomers and met-SWNT (18,0). Optimized geometry of the complex formed between DPP3T (top) or DPP4T (bottom) and SWNT (18,0). The long branched chains are replaced by methyl groups for simplicity. c) DPP polymers with four thiophene units in backbone.

on the above theoretical consideration, we design an investigation here to study the effect of the ratios of 4Ts in the DPP polymer backbone on sc-SWNT sorting. Here with the same side chains, polymer PDPP3T, PDPP3T-10T, PDPP3T-20T, and PDPP3T-40T with 0%, 10 mol%, 20 mol%, and 40 mol% of 4T, respectively, are designed to gradually enhance the electronic interactions between conjugated polymer and SWNT (Figure 1a). We note that PDPP4T with shorter side chains of 2-hexyldecyl ( $-\text{CHCH}(\text{C}_6\text{H}_{13})(\text{C}_8\text{H}_{17})$ ) has low solubility in toluene used for sorting. Therefore, to investigate the effect of side chains, we additionally prepared PDPP4Ts with longer branched side chains (Figure 1c).

Arc-discharged SWNTs (AD-SWNTs) (contain 70 wt% SWNTs according to the vendor) with diameters in the range of 1.1–1.8 nm were used for this work. After tip-sonicating a mixture of the polymer and AD-SWNTs in toluene for 30 min, the mixture was centrifuged for 30 min to remove nondispersible matters, such as metallic tubes, tube bundles, and amorphous carbons. Then the supernatant was collected for subsequent characterizations and device fabrication. For initial screening, a polymer/AD-SWNT ratio of 5 mg/5 mg in 25 mL toluene

was used. Figure 2a displays the second interband absorption of SWNTs ( $S_{22}$ : 900–1250 nm) of the sorted solutions (see Figure S1, Supporting Information, for the polymer absorption and Figure S2, Supporting Information, for the full absorption spectrum of polymer wrapped SWNTs). All the polymers showed dispersion ability for larger-diameter sc-SWNTs but the yield varied. As thiophenes were introduced from PDPP3T to PDPP3T-40T, the amount of dispersed sc-SWNTs increased accordingly, as evidenced from the higher absorption intensity at the  $S_{22}$  region of the supernatant.

To estimate the purity of the sorted tubes, we removed the polymers by thermally annealing polymer-SWNT films at 500 °C under Ar. This method has been demonstrated to be an effective way to eliminate the absorption interference from polymers without altering the electronic and optical properties of the SWNTs.<sup>[20,23]</sup> The absorption ratios between the first interband absorption of met-SWNTs ( $M_{11}$ : 600–800 nm) and the  $S_{22}$  can be used to qualitatively determine the relative amount of met-SWNT remaining in the sorted tubes. As shown in Figure 2b, after introducing more thiophenes in the polymer backbone, the absorption intensity of  $M_{11}$  band decreased

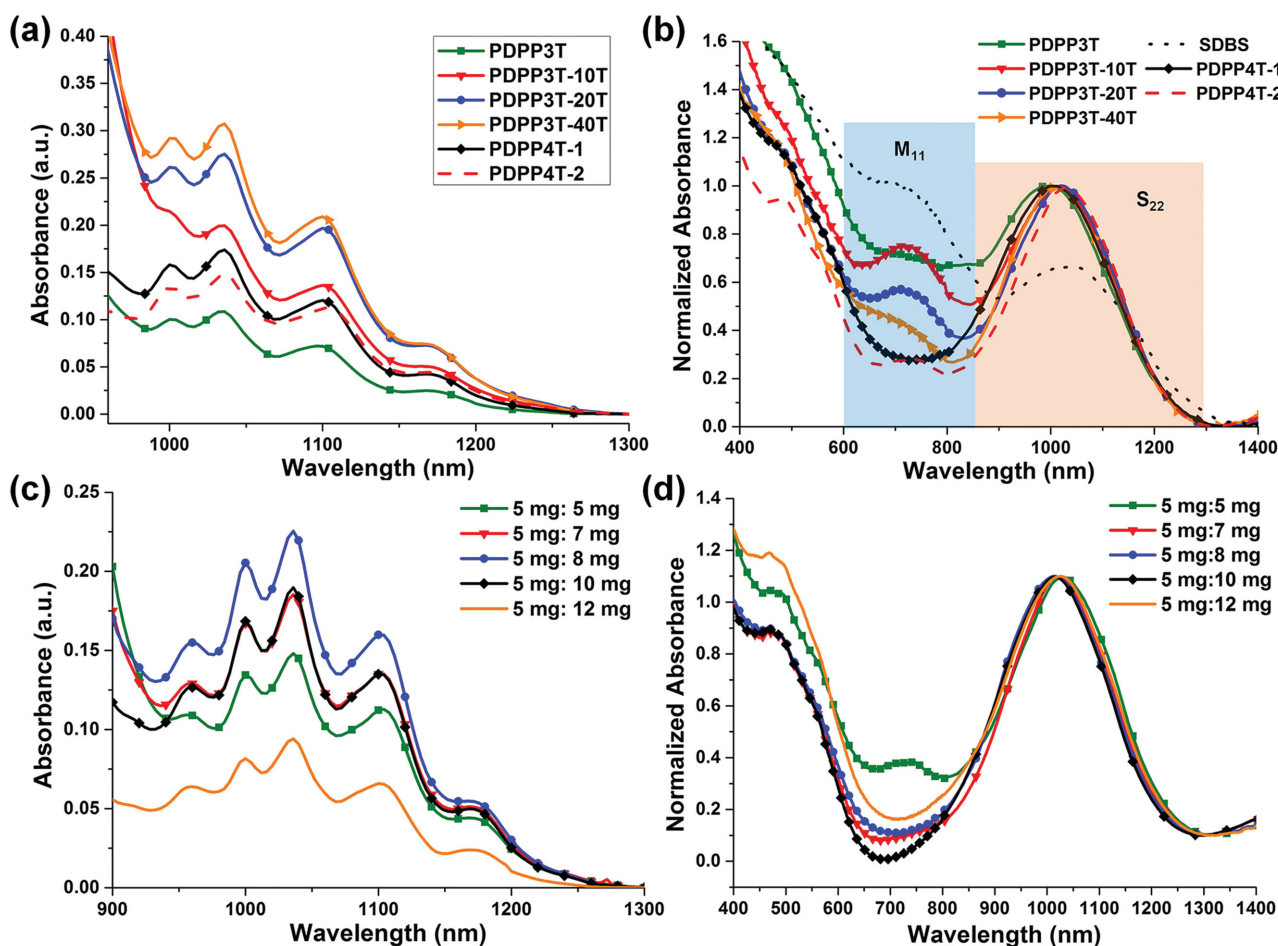


**Figure 2.** Absorption spectra of sc-SWNTs dispersed with DPP polymers. a) Different DPP polymers are used. Dispersing was carried out under the same ratio and conditions (polymer: AD-SWNT ratio: 5 mg:5 mg). b) Normalized absorption spectra of the sorted SWNTs after polymer removal. c) sc-SWNTs dispersed by PDPP4T-2 with various polymer: AD-SWNT ratios. d) Normalized absorption spectra of the PDPP4T-2 sorted SWNTs under various polymer: AD-SWNT ratios.

significantly. These results indicate that introducing more thiophenes in the polymer backbone can simultaneously increase both the dispersion yield and selectivity for large-diameter sc-SWNTs. After incorporating more thiophene units, polymer/SWNT complex exhibited stronger interactions. The stronger interactions between polymer and sc-SWNT resulted in higher dispersion yield, while the stronger interactions between polymer and met-SWNT led to increased charge transfer interactions and thereby higher selectivity.

Based on these results, we synthesized two additional polymers, PDPP4T-1 and PDPP4T-2, containing four thiophene units ( $n = 0, m = 100\%$ ) in the backbone, to further improve the selectivity for sc-SWNTs. Longer alkyl side chains are used in both polymers for good solubility, as shorter side chains result in severe polymer aggregation, which prevents effective polymer-SWNT interactions. Using the same sorting conditions, PDPP4T-1 and PDPP4T-2 clearly showed increased selectivity as indicated by the “deep valley” in the  $M_{11}$  absorption region (Figure 2b). PDPP4T polymers showed lower dispersion concentration than PDPP3T-10T under the same conditions (Figure 2a), as indicated by the relatively low  $S_{22}$  absorption, which is probably due to their lower solubility than the PDPP3T polymers.

Polymer/SWNT ratio is an important factor that affects the selectivity.<sup>[11c]</sup> Thus, we optimized the sorting conditions by varying the polymer/AD-SWNT ratios. Figure 2c displays the dispersion concentration changes of the PDPP4T-2 sorted SWNTs using various polymer/AD-SWNT ratios. As the AD-SWNT amount increases while keeping a constant polymer amount,

the dispersion concentration first increased and then decreased. The decrease in the dispersion concentration can be attributed to the absorption of the polymers by the excessive carbonaceous sediment, which then decreased the available polymer concentration for sorting in solution. The sorting selectivity is also dependent on the polymer/AD-SWNT ratio (Figure 2d). For polymer PDPP4T-2, a polymer/SWNT ratio of 5 mg/10 mg showed the highest selectivity. The estimated yield based on the SWNT amount in the starting materials for the sorted sc-SWNT was  $\approx 7\%$ . PDPP4T-1 also showed good dispersion ability and high selectivity (Figure S3, Supporting Information), but its selectivity is slightly inferior to PDPP4T-2 (Figure S4, Supporting Information).

## 2.2. Raman and Photoluminescence Excitation (PLE) Characterization of Sorted SWNTs

Raman spectroscopy was used to further validate the purity of the sorted sc-SWNTs. To exclude interference from the residue polymers, we removed the polymers by thermal annealing before measurements. Again, our previous work showed that the polymer removal process does not alter the SWNTs.<sup>[20]</sup> For unsorted AD-SWNTs, a strong radial-breathing-mode (RBM) peak of metallic tubes at  $151\text{ cm}^{-1}$  was observed (Figure 3a). After sorting with PDPP4T-2, this peak is almost invisible. In the G peak region ( $1500\text{--}1600\text{ cm}^{-1}$ ), the intensity of  $G^-$  peaks from met-SWNTs at  $1550\text{ cm}^{-1}$  significantly decreased, whereas the  $G^-$  peaks from sc-SWNTs at  $1570\text{ cm}^{-1}$  remained almost

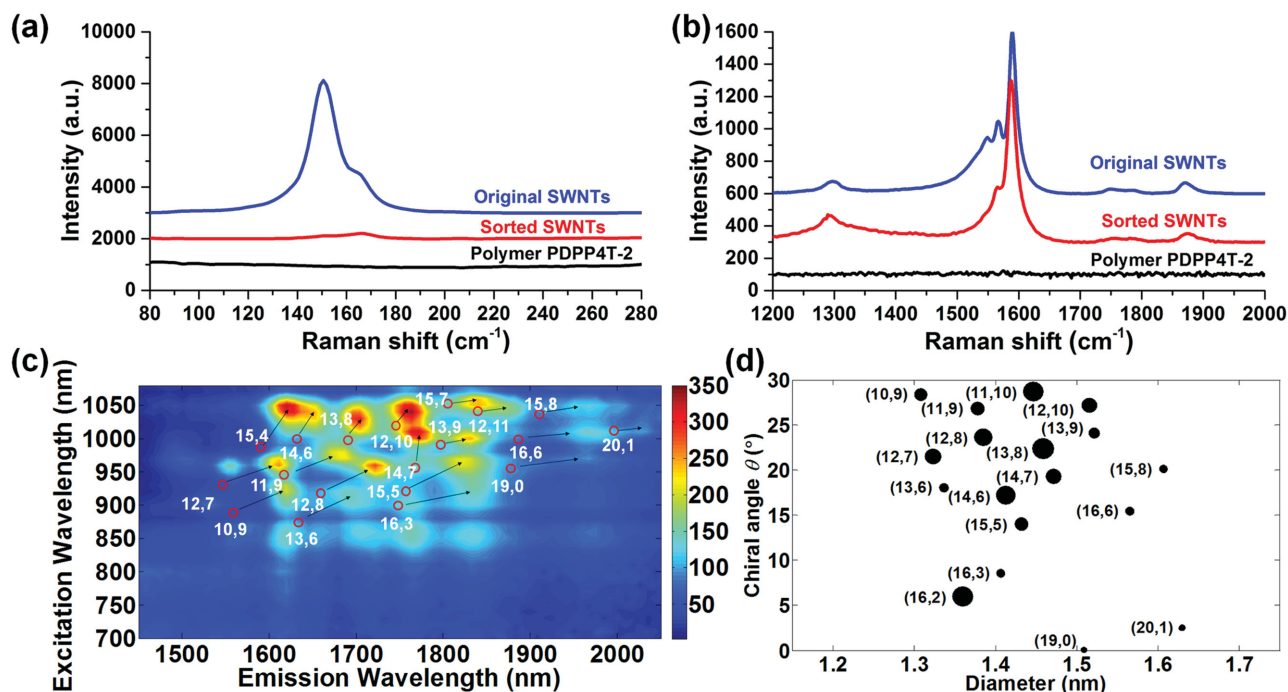


**Figure 3.** Raman and PLE characterization of DPP-sorted SWNTs. a,b) Raman spectra of pristine SWNTs, SWNTs sorted by PDPP4T-2, and polymer PDPP4T-2 excited using 785 nm laser. For sorted SWNTs, polymers were removed by thermal annealing in Ar. c) PLE maps of SWNTs dispersed by the PDPP4T-2 polymers. The circles indicate theoretical positions of sc-SWNT chiralities. A systematic redshift of the peaks was observed, which was attributed to dielectric screening caused by the interaction between polymer and SWNT. d) Chiral angle ( $\theta$ ) versus diameter ( $\varnothing$ ) ( $\theta/\varnothing$ ) map of SWNTs dispersed by PDPP4T-2. The circle areas are proportional to the concentration of the single species of SWNTs in the dispersion.

unchanged (Figure 3b). Using other excitation wavelengths (532 and 633 nm), the removal of met-SWNTs was further confirmed (Figures S5 and S6, Supporting Information). Compared with unsorted SWNTs, fewer RBM peaks from the sc-SWNTs remained in the sorted tubes, indicating that the polymer selectively disperses certain SWNT chiralities and diameters.

PLE mapping of dispersed SWNTs was used to determine the diameters and chiralities (Figure 3c), because this method can avoid the significant spectrum overlapping of different SWNT chiralities occurring in absorption spectroscopy.<sup>[24]</sup> Several strong peaks are assigned according to the theoretical prediction by Weisman et al.<sup>[25]</sup> (Figure 3d). As shown in the chiral angle ( $\theta$ ) versus diameter ( $\varnothing$ ) ( $\theta/\varnothing$ ) map, the sc-SWNTs dispersed by PDPP4T-2 are mainly around 1.5 nm. Some sc-SWNTs with diameters over 1.6 nm, such as (15,8) and (20,1), were also dispersed. The types of SWNTs dispersed are similar to our previous results for DPP-based polymers, probably due to their similar backbone structures.<sup>[20]</sup> Compared to conjugated polymers (e.g., polyfluorene and polythiophene based

polymers) that mainly disperse 1.3 nm sc-SWNTs with a weak dispersion ability for 1.5 nm sc-SWNTs,<sup>[11d,e,16,26]</sup> our results here again demonstrate that DPP-based polymers tend to disperse larger diameter SWNTs, likely attributed to their more planar DPP units and polymer backbones with stronger  $\pi$ - $\pi$  interactions. To further confirm the advantage of our DPP polymers, we prepared poly(3-dodecylthiophene-2,5-diyl) (P3DDT) dispersed sc-SWNTs using the same batch of crude AD-SWNTs. The PLE result showed that P3DDT mainly disperse SWNTs from 1.3 to 1.4 nm with a very weak dispersion ability of sc-SWNTs around 1.5 nm (Figure S7, Supporting Information).

### 2.3. Electrical Characterization of Sorted SWNTs

Figure 4a compares the absorption spectra of PDPP4T-2 sorted sc-SWNTs (this work), PDPP3T-10 sorted sc-SWNTs (the highest selectivity of our previous results),<sup>[20]</sup> and commercially available IsoNanotubes-S 99% sc-SWNTs (DGU method,

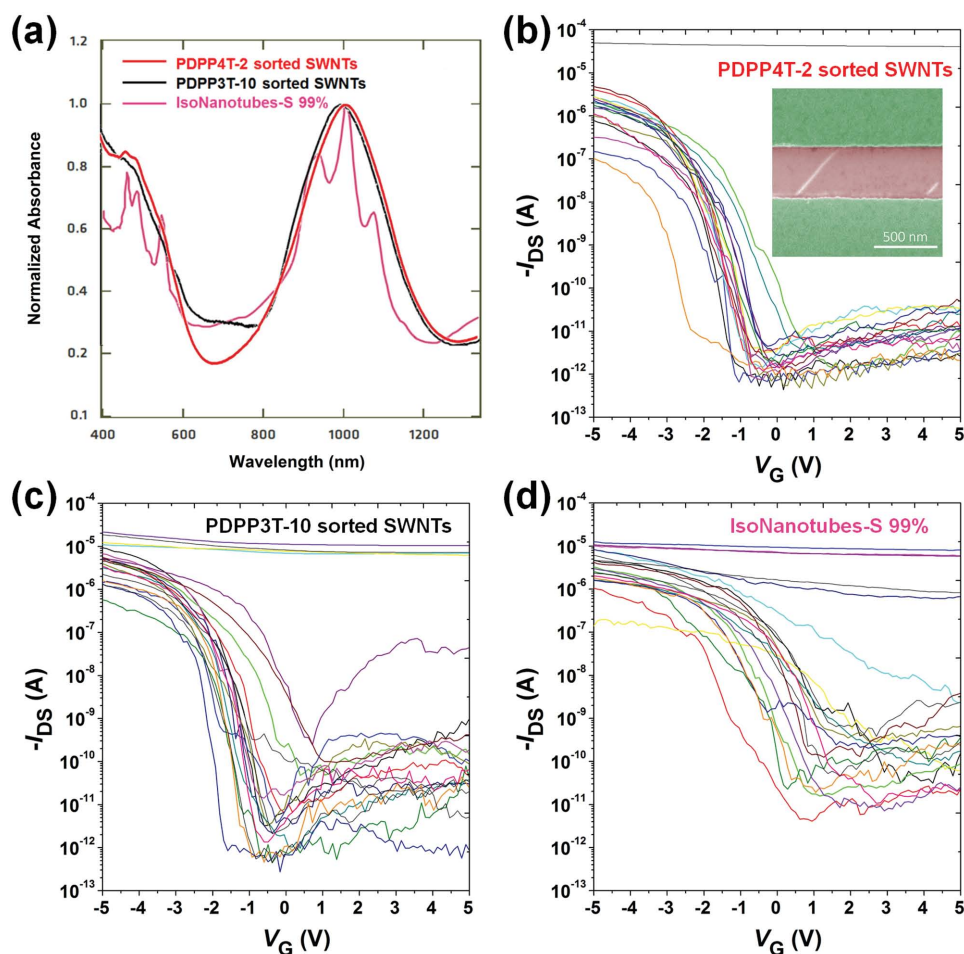


**Figure 4.** Characterization of sc-SWNT content in sorted tubes. a) Overlay of the absorption spectra of sc-SWNTs sorted by PDPP4T-2 and PDPP3T-10 with the absorption spectrum of the commercially available IsoNanotubes-S 99% SWNTs from Nanointegris Company. b) Short-channel devices based on sc-SWNTs sorted by PDPP4T-2. Eighteen devices with an average of 15 SWNTs per device were measured. Only one shorted device was observed. Inset is the SEM image of a short channel device. c) Short channel devices based on sc-SWNTs sorted by PDPP3T-10. Twenty one devices with an average of 8.75 SWNTs per device were measured. Four shorted devices were observed. d) Short-channel devices based on IsoNanotubes-S 99%. Twenty devices with an average of 7.5 SWNTs per device were measured. Five shorted devices were observed. Device configuration: Pd electrodes with  $L = 0.4 \mu\text{m}$  and  $W = 50 \mu\text{m}$ , dielectric layer: 42 nm  $\text{SiO}_2$ . Bias condition:  $V_{\text{DS}} = -1 \text{ V}$ .

product information provided by the vendor).<sup>[27]</sup> PDPP4T-2 sorted sc-SWNTs show higher selectivity as indicated by the “deep valley” in the  $M_{11}$  region. However, absorption spectroscopy cannot be used to quantify the selectivity.<sup>[14,18]</sup> To further substantiate the purity comparison, short channel FET devices with a channel length of 400 nm were fabricated on  $\text{SiO}_2$  (42 nm)/Si wafers (Figure 4b–d). For PDPP4T-2 sorted sc-SWNTs, one shorted device was observed in 18 devices chosen randomly. Each transistor contains on average 15 SWNTs, as characterized using scanning electron microscope (SEM) images. Since our semiconducting tube purity is high, we assume that any shorted devices were caused by one met-SWNT. Thus, the purity for PDPP4T-2 sorted sc-SWNT is estimated to be 99.6%, because only one device out of 18 was shorted with  $\approx 18 \times 15 = 270$  tubes were measured  $[(1 - 1/18 \times 15) \times 100\% = 99.6\%]$ . Similarly, the purity for PDPP3T-10 sorted sc-SWNTs and IsoNanotubes-S 99% SWNTs were estimated to be 97.8% [4 out of 21 devices were shorted,  $(1 - 4/21 \times 8.75) \times 100\% = 97.8\%$ ] and 96.7% [5 out of 20 devices were shorted,  $(1 - 5/20 \times 7.5) \times 100\% = 96.7\%$ ], respectively. These results agree well with the trend observed by the absorption spectra. In contrast, both DGU and column chromatography methods require long purification time (18–24 h) and multiple iterations to produce

high purity sc-SWNT with >99.5% purity measured by electrical measurements.<sup>[7,14]</sup> Compared to these methods, our method demonstrated here can rapidly produce large-diameter sc-SWNT with higher purity in 1 h.

To explore the application of our sorted sc-SWNTs in large-area TFTs, bottom-gate bottom-contact device configuration was used to fabricate random SWNT networks on  $\text{SiO}_2$  (300 nm)/Si wafers using the solution shearing method.<sup>[28]</sup> Compared to other fabrication methods, e.g., drop-casting and soaking,<sup>[11c,15s,23]</sup> solution shearing has the potential for large-area fabrication with better film uniformity (Figure 5a). A two-step shearing method was used: (1) the sorted SWNT solution was sheared onto a  $\text{SiO}_2$  (300 nm)/Si substrate at  $0.05 \text{ mm s}^{-1}$ ; (2) neat toluene was then sheared at  $0.1 \text{ mm s}^{-1}$  to remove most of the polymer residues. The SWNT network density is a critical parameter for TFT device performance.<sup>[29]</sup> By using solution shearing, device performance can be tuned by shearing speed, solution concentration and substrate temperature. Figure 5b and Figure S8 (Supporting Information) displays the atomic force microscopy (AFM) image showing a SWNT network with a tube density  $\approx 60 \text{ tubes } \mu\text{m}^{-2}$ . Most of the sorted tubes exhibited tube lengths in the range of 0.5–3  $\mu\text{m}$ . Under this condition, the FET devices exhibited high hole mobilities in the

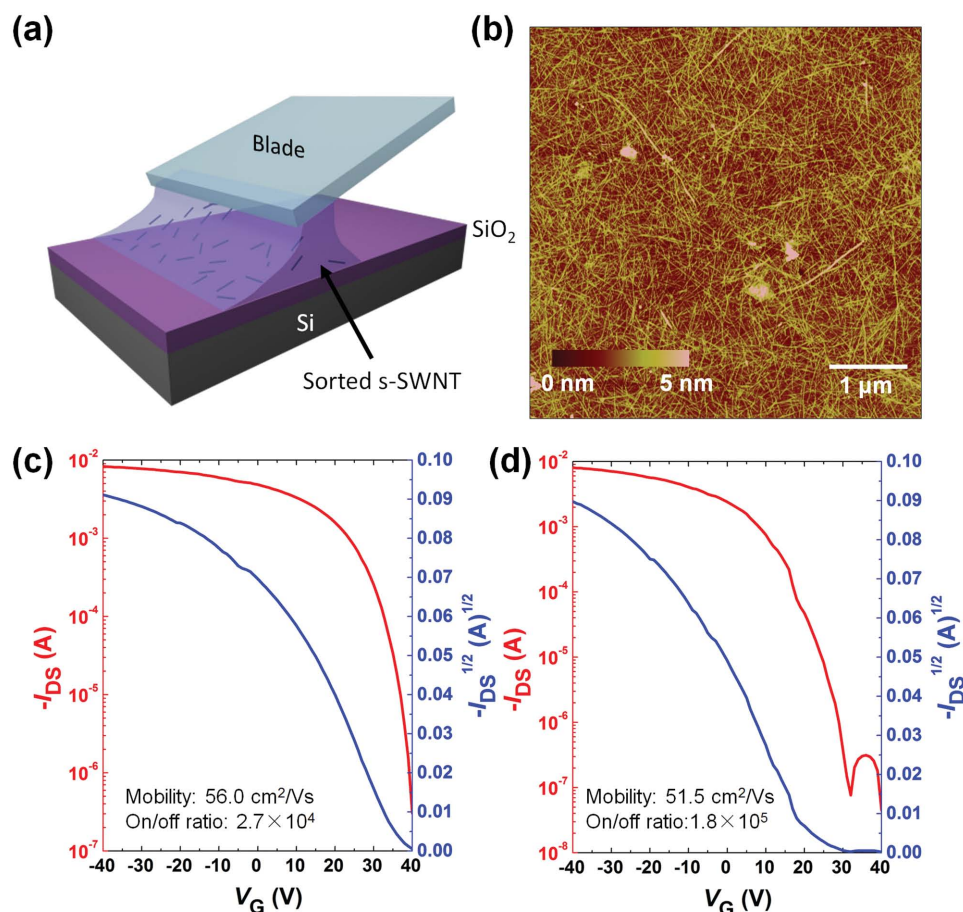


**Figure 5.** Thin film transistor performance of sorted SWNT networks. a) Schematic representation for SWNT TFTs fabricated by solution shearing method. b) AFM height images of SWNT network fabricated by solution shearing method. Transfer characteristics of the SWNT network TFTs measured c) in air and d) in  $\text{N}_2$  glove box. Device configuration:  $L = 30 \mu\text{m}$ ,  $W = 600 \mu\text{m}$ ,  $V_{DS} = -40 \text{ V}$ .

range of 41–57 cm<sup>2</sup> V<sup>-1</sup> s<sup>-1</sup> (average: 48.0 ± 6.0 cm<sup>2</sup> V<sup>-1</sup> s<sup>-1</sup>) with on/off ratios of 10<sup>4</sup>–10<sup>5</sup> (Figure 5c). The FET devices measured in air showed positive and large V<sub>i</sub> of 34–37 V, which is likely caused by oxygen/water doping or presence of traps.<sup>[30]</sup> When measuring the same devices in a N<sub>2</sub> glove box, the V<sub>i</sub> shifted to 15–22 V and the device can be completely turned off. The hole mobilities measured in a glove box are slightly lower in the range of 35–52 cm<sup>2</sup> V<sup>-1</sup> s<sup>-1</sup> with increased on/off ratios over 10<sup>5</sup>. This performance is among the highest for solution-processed random SWNT network TFTs.<sup>[7,11c,11e,15a,23,31]</sup> As a comparison, the unsorted SWNT devices fabricated under the same conditions showed on/off ratios lower than 10. When using bottom-gate top-contact configuration and Ti (2 nm)/Pd (30 nm) as electrodes, the FET devices showed good ambipolar transport behaviors due to the smaller bandgap of the sorted sc-SWNTs (Figure S9, Supporting Information). Compared with small-diameter tubes that show high on/off ratios >10<sup>6</sup>,<sup>[32]</sup> our on/off ratios are high because the theoretical on/off limits for 1D low-bandgap semiconductors with bandgaps of 0.6–0.8 eV are 2.7 × 10<sup>4</sup>–2.3 × 10<sup>6</sup>.<sup>[33]</sup> The high on/off ratio of our sorted sc-SWNTs further confirms the high purity of our sorted sc-SWNTs.

### 3. Conclusion

In summary, we have demonstrated improved selectivity for larger diameter (>1.4 nm) sc-SWNTs based on DPP polymers. After incorporation of more thiophene building blocks in DPP polymer backbones, both the selectivity and yield for sc-SWNTs were increased. To provide a quantitative comparison of the selectivity of sc-SWNTs sorted by different polymers and methods, short-channel FET devices were fabricated. Using our backbone-engineered DPP polymers, sc-SWNTs with high purity of 99.6% and large diameter (1.4–1.6 nm) close to the ideal tube diameter (1.7 nm) for high-performance computing can be obtained within 1 h of processing time. Our method demonstrates a fast, scalable, and high-purity SWNT sorting process, thus it is promising for high-performance electronic devices.

### 4. Experimental Section

**General Procedures for Sorting of sc-SWNTs:** PDPP4T-2 (5 mg) and AD-SWNTs (10 mg) (P2 SWNT purchased from Carbon Solutions, Inc, contains 70 wt% SWNTs) were mixed in 25 mL of toluene and ultrasonicated for 30 min at an amplitude level of 70% (Cole Parmer ultrasonicator 750 W) with a cooling bath (the inner tube temperature is around 40 °C). The mixture was then centrifuged at 17 000 rpm (22 000 g) for 30 min at 16 °C. The supernatant was collected and used for subsequent characterization.

To determine the sorting yield, a nylon membrane (0.2 μm pore size) covered with sorted sc-SWNT was prepared by filtering the supernatant through a filter. The nylon membrane was rinsed extensively with hot chloroform to remove any residue polymer. It was dried under vacuum and the weight to determine the yield of sorted sc-SWNTs as 7%. The yield is based on the weight ratio of sc-SWNTs and the SWNT content in raw AD-SWNT (70 wt% SWNTs and 30 wt% amorphous carbons/catalysts as provided by the vendor).

**Sorted SWNT Characterization:** The dispersion concentration was evaluated by UV–vis–NIR measurements using a 1 cm path-length quartz

cell. To determine the selectivity, sc-SWNT thin films were prepared by drop-casting the supernatants on glass substrates and annealing the film at 500 °C under Ar for 1 h to remove the residue polymer. Raman spectroscopy was carried out at 2.33 eV (532 nm), 1.93 eV (638 nm), and 1.58 eV (785 nm) excitation at ×100 magnification and 1-μm spot size. The peak positions were calibrated with the Si line at 521 cm<sup>-1</sup>. The PLE spectra of various SWNT samples in toluene were taken according to our previous reported method.<sup>[20]</sup>

**Short Channel Device Fabrication and Characterization:** Drop-cast diluted SWNT solutions (ten times dilute) on thermally grown SiO<sub>2</sub> (42 nm)/Si wafer, wait 20 s, then gradually ramp spin speed to 3000 RPM until the surface is dry. Removal of wrapping polymers from SWNTs was carried out through rapid thermal annealing (RTA) of wafer for 15 min in N<sub>2</sub> at 500 °C. To ensure no oxygen was present during RTA, the chamber was purged before annealing. Palladium (30 nm) as metal contact was defined by traditional photolithography process using an ASML 5500 Stepper. Using a chuck to globally bias the wafer as a gate, the electrical behavior of the carbon nanotubes was measured using an Agilent 4156C.

**TFT Fabrication and Characterization:** The drain and source electrodes for bottom-contact device electrodes were fabricated on a heavily doped 4 in. silicon wafer with 300 nm SiO<sub>2</sub> by photolithography. A bilayer of Cr (3 nm) and Au (40 nm) was deposited by thermal evaporation as the source-drain electrodes, followed by a lift-off process in acetone. For solution shearing method, sorted SWNT solution (20 μL) was first sheared at a speed of 0.05 mm s<sup>-1</sup>. Then neat toluene (20 μL) was sheared at a speed of 0.1 mm s<sup>-1</sup> to remove most of the residue polymers. The processes were performed at room temperature under air. For PDPP4T-2 sorted sc-SWNT solutions, repeating the two shearing steps three to five times provides enough tube density for charge carrier percolation. The device was then rinsed with toluene, dried with nitrogen flow, and annealed at 200 °C for 20 min. The devices were then soaked in hot toluene (80 °C) for 2 h to remove the wrapping polymers (Figure S8, Supporting Information). Then the devices were annealed again at 200 °C for 20 min to remove solvent residues. The evaluations of the TFTs were carried out in atmosphere on a probe station. The carrier mobility, μ, was calculated from the data in the saturated regime according to the equation I<sub>SD</sub> = (W/2L)C<sub>i</sub>μ(V<sub>G</sub> - V<sub>T</sub>)<sup>2</sup>, where C<sub>i</sub> = 11 nF cm<sup>-2</sup>. The mobilities were obtained using a channel length of 20 or 30 μm with W/L = 20.

### Supporting Information

Supporting Information is available from the Wiley Online Library or from the author.

### Acknowledgements

The authors thank Dr. Igor Porchorovski, Dr. Ying-Chih Lai, Dr. Huiliang Wang, and Dr. Jeffrey B.-H. Tok for discussions.

Received: September 9, 2015

Revised: September 21, 2015

Published online: October 31, 2015

- [1] a) M. M. Shulaker, G. Hills, N. Patil, H. Wei, H.-Y. Chen, H. S. P. Wong, S. Mitra, *Nature* **2013**, 507, 526; b) H. Chen, Y. Cao, J. Zhang, C. Zhou, *Nat. Commun.* **2014**, 5, 4097.
- [2] A. Javey, J. Guo, Q. Wang, M. Lundstrom, H. Dai, *Nature* **2003**, 424, 654.
- [3] a) M. E. Itkis, F. Borondics, A. Yu, R. C. Haddon, *Science* **2006**, 312, 413; b) Y. Ye, D. J. Bindl, R. M. Jacobberger, M.-Y. Wu, S. S. Roy, M. S. Arnold, *Small* **2014**, 10, 3299.

- FULL PAPER**
- [4] a) C. Wang, D. Hwang, Z. Yu, K. Takei, J. Park, T. Chen, B. Ma, A. Javey, *Nat. Mater.* **2013**, *12*, 899; b) F. Xu, M.-Y. Wu, N. S. Safron, S. S. Roy, R. M. Jacobberger, D. J. Bindl, J.-H. Seo, T.-H. Chang, Z. Ma, M. S. Arnold, *Nano Lett.* **2014**, *14*, 682.
- [5] M. C. Hersam, *Nat. Nanotechnol.* **2008**, *3*, 387.
- [6] H. Zhang, B. Wu, W. Hu, Y. Liu, *Chem. Soc. Rev.* **2011**, *40*, 1324.
- [7] M. S. Arnold, A. A. Green, J. F. Hulvat, S. I. Stupp, M. C. Hersam, *Nat. Nanotechnol.* **2006**, *1*, 60.
- [8] Y. Miyata, K. Shiozawa, Y. Asada, Y. Ohno, R. Kitaura, T. Mizutani, H. Shinohara, *Nano Res.* **2011**, *4*, 963.
- [9] R. Krupke, F. Hennrich, H. v. Löhneysen, M. M. Kappes, *Science* **2003**, *301*, 344.
- [10] X. Tu, S. Manohar, A. Jagota, M. Zheng, *Nature* **2009**, *460*, 250.
- [11] a) A. Nish, J.-Y. Hwang, J. Doig, R. J. Nicholas, *Nat. Nanotechnol.* **2007**, *2*, 640; b) S. K. Samanta, M. Fritsch, U. Scherf, W. Gomulya, S. Z. Bisri, M. A. Loi, *Acc. Chem. Res.* **2014**, *47*, 2446; c) J. Ding, Z. Li, J. Lefebvre, F. Cheng, G. Dubey, S. Zou, P. Finnie, A. Hrdina, L. Scoles, G. P. Lopinski, C. T. Kingston, B. Simard, P. R. L. Malenfant, *Nanoscale* **2014**, *6*, 2328; d) K. S. Mistry, B. A. Larsen, J. L. Blackburn, *ACS Nano* **2013**, *7*, 2231; e) W. Gomulya, G. D. Costanzo, E. J. F. de Carvalho, S. Z. Bisri, V. Derenskiy, M. Fritsch, N. Fröhlich, S. Allard, P. Gordiichuk, A. Herrmann, S. J. Marrink, M. C. dos Santos, U. Scherf, M. A. Loi, *Adv. Mater.* **2013**, *25*, 2948.
- [12] G. S. Tulevski, A. D. Franklin, D. Frank, J. M. Lobe, Q. Cao, H. Park, A. Afzali, S.-J. Han, J. B. Hannon, W. Haensch, *ACS Nano* **2014**, *8*, 8730.
- [13] Z. Chen, J. Appenzeller, J. Knoch, Y.-m. Lin, P. Avouris, *Nano Lett.* **2005**, *5*, 1497.
- [14] G. S. Tulevski, A. D. Franklin, A. Afzali, *ACS Nano* **2013**, *7*, 2971.
- [15] a) H. W. Lee, Y. Yoon, S. Park, J. H. Oh, S. Hong, L. S. Liyanage, H. Wang, S. Morishita, N. Patil, Y. J. Park, J. J. Park, A. Spakowitz, G. Galli, F. Gygi, P. H. S. Wong, J. B. H. Tok, J. M. Kim, Z. Bao, *Nat. Commun.* **2011**, *2*, 541; b) F. Jakubka, S. P. Schießl, S. Martin, J. M. Englert, F. Hauke, A. Hirsch, J. Zaumseil, *ACS Macro Lett.* **2012**, *1*, 815; c) N. Berton, F. Lemasson, J. Tittmann, N. Stürzl, F. Hennrich, M. M. Kappes, M. Mayor, *Chem. Mater.* **2011**, *23*, 2237.
- [16] M. Tange, T. Okazaki, S. Iijima, *J. Am. Chem. Soc.* **2011**, *133*, 11908.
- [17] M. P. Ramuz, M. Vosgueritchian, P. Wei, C. Wang, Y. Gao, Y. Wu, Y. Chen, Z. Bao, *ACS Nano* **2012**, *6*, 10384.
- [18] W.-J. Kim, C. Y. Lee, K. P. O'Brien, J. J. Plombon, J. M. Blackwell, M. S. Strano, *J. Am. Chem. Soc.* **2009**, *131*, 3128.
- [19] S. Park, H. W. Lee, H. Wang, S. Selvarasah, M. R. Dokmeci, Y. J. Park, S. N. Cha, J. M. Kim, Z. Bao, *ACS Nano* **2012**, *6*, 2487.
- [20] T. Lei, Y.-C. Lai, G. Hong, H. Wang, P. Hayoz, R. T. Weitz, C. Chen, H. Dai, Z. Bao, *Small* **2015**, *11*, 2946.
- [21] a) Y. Kanai, J. C. Grossman, *Nano Lett.* **2008**, *8*, 908; b) J. M. Holt, A. J. Ferguson, N. Kopidakis, B. A. Larsen, J. Bult, G. Rumbles, J. L. Blackburn, *Nano Lett.* **2010**, *10*, 4627.
- [22] H. Wang, B. Hsieh, G. Jiménez-Osés, P. Liu, C. J. Tassone, Y. Diao, T. Lei, K. N. Houk, Z. Bao, *Small* **2014**, *11*, 126.
- [23] H. Wang, J. Mei, P. Liu, K. Schmidt, G. Jiménez-Osés, S. Osuna, L. Fang, C. J. Tassone, A. P. Zoombelt, A. N. Sokolov, K. N. Houk, M. F. Toney, Z. Bao, *ACS Nano* **2013**, *7*, 2659.
- [24] K. Iakoubovskii, N. Minami, S. Kazaoui, T. Ueno, Y. Miyata, K. Yanagi, H. Kataura, S. Ohshima, T. Saito, *J. Phys. Chem. B* **2006**, *110*, 17420.
- [25] R. B. Weisman, S. M. Bachilo, *Nano Lett.* **2003**, *3*, 1235.
- [26] C. Wang, L. Qian, W. Xu, S. Nie, W. Gu, J. Zhang, J. Zhao, J. Lin, Z. Chen, Z. Cui, *Nanoscale* **2013**, *5*, 4156.
- [27] The spectrum was adapted from Nanointegris website, <http://www.nanointegris.com/en/semiconducting> (accessed: July 2015).
- [28] G. Giri, E. Verploegen, S. C. B. Mannsfeld, S. Atahan-Evrenk, D. H. Kim, S. Y. Lee, H. A. Becerril, A. Aspuru-Guzik, M. F. Toney, Z. Bao, *Nature* **2011**, *480*, 504.
- [29] D.-m. Sun, M. Y. Timmermans, Y. Tian, A. G. Nasibulin, E. I. Kauppinen, S. Kishimoto, T. Mizutani, Y. Ohno, *Nat. Nanotechnol.* **2011**, *6*, 156.
- [30] N. M. Dissanayake, Z. Zhong, *Nano Lett.* **2011**, *11*, 286.
- [31] a) S. Z. Bisri, J. Gao, V. Derenskiy, W. Gomulya, I. Iezhokin, P. Gordiichuk, A. Herrmann, M. A. Loi, *Adv. Mater.* **2012**, *24*, 6147; b) T. Takahashi, K. Takei, A. G. Gillies, R. S. Fearing, A. Javey, *Nano Lett.* **2011**, *11*, 5408; c) M. C. LeMieux, M. Roberts, S. Barman, Y. W. Jin, J. M. Kim, Z. Bao, *Science* **2008**, *321*, 101; d) H. Okimoto, T. Takenobu, K. Yanagi, Y. Miyata, H. Shimotani, H. Kataura, Y. Iwasa, *Adv. Mater.* **2010**, *22*, 3981; e) G. J. Brady, Y. Joo, S. Singha Roy, P. Gopalan, M. S. Arnold, *Appl. Phys. Lett.* **2014**, *104*, 083107; f) M. Engel, J. P. Small, M. Steiner, M. Freitag, A. A. Green, M. C. Hersam, P. Avouris, *ACS Nano* **2008**, *2*, 2445; g) M. Shimizu, S. Fujii, T. Tanaka, H. Kataura, *J. Phys. Chem. C* **2013**, *117*, 11744.
- [32] V. Derenskiy, W. Gomulya, J. M. S. Rios, M. Fritsch, N. Fröhlich, S. Jung, S. Allard, S. Z. Bisri, P. Gordiichuk, A. Herrmann, U. Scherf, M. A. Loi, *Adv. Mater.* **2014**, *26*, 5969.
- [33] Y. Zhao, D. Candebat, C. Delker, Y. Zi, D. Janes, J. Appenzeller, C. Yang, *Nano Lett.* **2012**, *12*, 5331.